EPJ Web of Conferences **175**, 06009 (2018) https://doi.org/10.1051/epjconf/201817506009
Lattice 2017

Bethe-Salpeter wave functions of η_c(1S, 2S) and ψ(1S, 2S) states: local-potential description of the charmonium system revisited

Kazuki Nochi[1,⋆], *Taichi* Kawanai[2], and *Shoichi* Sasaki[1]

[1] *Department of Physics, Tohoku University, Sendai 980-8578, Japan*
[2] *Jülich Supercomputing Center, Jülich D-52425, German*

Abstract. The quark potential models with an energy-independent central potential have been successful for understanding the conventional charmonium states especially below the open charm threshold. As one might consider, however, the interquark potential is in general energy-dependent, and its tendency gets stronger in higher lying states. Confirmation of whether the interquark potential is energy-independent is also important to verify the validity of the quark potential models. In this talk, we examine the energy dependence of the charmonium potential, which can be determined from the Bethe-Salpeter (BS) amplitudes of $c\bar{c}$ mesons in lattice QCD. We first calculate the BS amplitudes of radially excited charmonium states, the $\eta_c(2S)$ and $\psi(2S)$ states, using the variational method and then determine both the quark kinetic mass and the charmonium potential within the HAL QCD method. Through a direct comparison of charmonium potentials determined from both the $1S$ and $2S$ states, we confirm that neither the central nor spin-spin potential shows visible energy dependence at least up to $2S$ state.

1 Introduction

The constituent quark description has been successful in qualitatively understanding properties of the charmonium and bottomonium states, especially below the thresholds for decays to mesons with open heavy flavor [1–3]. In quark potential models, essential features of the QCD quark-gluon dynamics are encoded in the interquark potential. For the heavy quarkonium system, the Cornell potential, which consists of the Coulomb and linear terms, is often adopted. Although the Cornell potential was not directly derived from QCD, the functional form has been qualitatively justified by the static heavy quark potential obtained from Wilson loops in lattice QCD [4]. However, the static potential is defined in the infinitely heavy quark limit.

An interesting idea to define a two-body potential from the equal-time Bethe-Salpeter (BS) amplitude, which is called the BS wave function in the rest frame, was proposed by Aoki, Hatsuda and Ishii for studying the nuclear force in lattice QCD [5, 6]. Subsequently, Ikeda and Iida applied the same idea to the quarkonium system in order to compute the interquark potential without the adiabatic approximation [7, 8]. These preceding studies led us to propose a novel approach, where both the quark kinetic mass and the interquark potential are self-consistently determined within the BS amplitude method, in order to obtain *proper interquark potential at finite quark mass* using lattice QCD [9].

⋆ Speaker, e-mail: nochi@nucl.phys.tohoku.ac.jp

We have elaborated the new approach to determine reliable interquark potential from lattice QCD in our previous works [9–12]. Now, we naturally have the question whether a universal interquark potential and a unique quark mass can be simultaneously defined in a series of the BS amplitudes from the ground state to excited states. In this work, we extend the BS amplitude method to the radially excited charmonium mesons. Comparing the interquark potential of the ground state with the one of the radially excited state, we will answer the above question later.

2 Formalism

2.1 Quark kinetic mass and interquark potential from BS wave functions

In this section, we briefly describe how to determine the quark kinetic mass and the interquark potential from the BS amplitudes in lattice QCD. In our preceding studies, the quark kinetic mass m_Q has been read off from the long-distance asymptotic value of the difference of "quantum kinetic energies" between the spin-singlet (PS) and -triplet (V) states in the hyperfine multiplet for the $1S$ states [9–12]. We here generalize this idea to nS states. The quark kinetic mass can be determined from a set of the nS wave functions $\phi_\Gamma^{nS}(r)$ for $\Gamma = \mathrm{PS}, \mathrm{V}$ in the following way [9]:

$$m_Q(nS) = \lim_{r\to\infty} \frac{-1}{E_{\mathrm{hyp}}(nS)} \left\{ \frac{\boldsymbol{\nabla}^2 \phi_{\mathrm{V}}^{nS}(r)}{\phi_{\mathrm{V}}^{nS}(r)} - \frac{\boldsymbol{\nabla}^2 \phi_{\mathrm{PS}}^{nS}(r)}{\phi_{\mathrm{PS}}^{nS}(r)} \right\} \tag{1}$$

with the hyperfine splitting energy of the nS states, $E_{\mathrm{hyp}}(nS) = M_{\mathrm{V}}(nS) - M_{\mathrm{PS}}(nS)$. The derivative $\boldsymbol{\nabla}^2$ appeared in Eq. (1) is defined by the discrete Laplacian on the lattice. As shown in Ref. [11], a suitable choice of the discrete Laplacian is defined in the discrete polar coordinates in order to reduce the discretization artifacts on the short-range behavior of the interquark potential.

The interquark potential for S-wave states can be decomposed into the central (spin-independent) potential $V_{\mathrm{C}}(r)$ and the spin-spin potential $V_{\mathrm{S}}(r)$, which are defined by the BS wave functions of nS states, $\phi_{\mathrm{PS}}^{nS}(r)$ and $\phi_{\mathrm{V}}^{nS}(r)$, as below:

$$V_{\mathrm{C}}^{nS}(r) = E_{\mathrm{ave}}(nS) + \frac{1}{m_Q(nS)} \left\{ \frac{3}{4} \frac{\boldsymbol{\nabla}^2 \phi_{\mathrm{V}}^{nS}(r)}{\phi_{\mathrm{V}}^{nS}(r)} + \frac{1}{4} \frac{\boldsymbol{\nabla}^2 \phi_{\mathrm{PS}}^{nS}(r)}{\phi_{\mathrm{PS}}^{nS}(r)} \right\} \tag{2}$$

and

$$V_{\mathrm{S}}^{nS}(r) = E_{\mathrm{hyp}}(nS) + \frac{1}{m_Q(nS)} \left\{ \frac{\boldsymbol{\nabla}^2 \phi_{\mathrm{V}}^{nS}(r)}{\phi_{\mathrm{V}}^{nS}(r)} - \frac{\boldsymbol{\nabla}^2 \phi_{\mathrm{PS}}^{nS}(r)}{\phi_{\mathrm{PS}}^{nS}(r)} \right\} \tag{3}$$

where $E_{\mathrm{ave}}(nS) = M_{\mathrm{ave}}(nS) - 2m_Q(nS)$. The mass $M_{\mathrm{ave}}(nS)$ denotes the spin-averaged mass for the nS states as $\frac{3}{4}M_{\mathrm{V}}(nS) + \frac{1}{4}M_{\mathrm{PS}}(nS)$.

To obtain the nS wave functions, we use the BS amplitude method combined with the variational method [13, 14]. Details of how to determine the BS wave functions with the variational method are described in Ref. [15].

2.2 "time-dependent" method for the interquark potential

The original method developed by the HAL QCD Collaboration [5, 6] starts from the fact that the BS wave function satisfies the "stationary" Schrödinger equation with a nonlocal and energy-independent potential below the inelastic threshold [6]. We simply apply this method to quark-antiquark ($Q\bar{Q}$) system. Under an assumption that there is an energy-independent nonlocal potential

even in the $Q\bar{Q}$ system [15], let us consider the following "time-independent" Schrödinger equation for the BS wave function ϕ_Γ in the non-relativistic approximation:

$$\left\{E_\Gamma + \frac{\boldsymbol{\nabla}^2}{m_Q}\right\}\phi_\Gamma(\boldsymbol{r}) = \int d\boldsymbol{r}' U(\boldsymbol{r},\boldsymbol{r}')\phi_\Gamma(\boldsymbol{r}'), \tag{4}$$

where $E_\Gamma = M_\Gamma - 2m_Q$. As discussed in Ref [9, 10], for the S-wave meson states, the local potentials $V_{\rm PS}(r)$ and $V_{\rm V}(r)$ defined at the leading order of the velocity expansion: $U(\boldsymbol{r},\boldsymbol{r}') = \left\{V_{\rm PS(V)}(r) + O(v^2)\right\}\delta^2(\boldsymbol{r}-\boldsymbol{r}')$ with $v = |\boldsymbol{\nabla}/m_Q|$, is given by

$$V_{\rm PS(V)}(r) = E_{\rm PS(V)} + \frac{1}{m_Q}\frac{\boldsymbol{\nabla}^2\phi_{\rm PS(V)}(r)}{\phi_{\rm PS(V)}(r)}\ . \tag{5}$$

The interquark potential $V_{\rm PS(V)}(r)$ can be written by $V_{\rm PS(V)}(r) = V_{\rm C}(r) + (\boldsymbol{S}_Q\cdot\boldsymbol{S}_{\bar{Q}})V_{\rm S}(r)$, where the spin operator $\boldsymbol{S}_Q\cdot\boldsymbol{S}_{\bar{Q}}$ may be replaced by expectation value of $-3/4(1/4)$ for the PS(V) state. Then, $V_{\rm C}(r)$ and $V_{\rm S}(r)$ are separately obtained as shown in Eqs. (2) and (3).

Starting with no explicit energy dependence on the non-local potential, the HAL QCD Collaboration has proposed an alternative method to derive the hadron-hadron interactions by so-called "time-dependent" Schrödinger-like equation [16], instead of Eq. (4). Here, we also may apply the new method to our interest $Q\bar{Q}$ system. For this purpose, let us introduce the following correlation function:

$$R_\Gamma(\boldsymbol{r},t) = C_\Gamma(\boldsymbol{r},t)/(e^{-m_Q t})^2, \tag{6}$$

where $C_\Gamma(\boldsymbol{r},t)$ is the $\boldsymbol{r}$-dependent two-point correlation function:

$$C_\Gamma(\boldsymbol{r},t) = \sum_{\boldsymbol{x},\boldsymbol{x}'} = \langle 0|\bar{Q}(\boldsymbol{x},t)\Gamma Q(\boldsymbol{x}+\boldsymbol{r},t)(\bar{Q}(\boldsymbol{x}',0)\Gamma Q(\boldsymbol{x}',0))^\dagger|0\rangle. \tag{7}$$

Here, m_Q denotes the quark kinetic mass that should be determined in advance as described in Eq. (1).

Considering the time derivative, $\frac{\partial}{\partial t}R_\Gamma(\boldsymbol{r},t)$, with the help of the spectral decomposition of the original $\boldsymbol{r}$-dependent correlation function $C_\Gamma(\boldsymbol{r},t)$, we then arrive at the "time-dependent" Schrödinger-like equation for the $Q\bar{Q}$ system [16] as well,

$$\left\{\frac{1}{4m_Q}\frac{\partial^2}{\partial t^2} - \frac{\partial}{\partial t} + \frac{\boldsymbol{\nabla}^2}{m_Q}\right\}R_{\rm PS(V)}(\boldsymbol{r},t) = \int d\boldsymbol{r}' U(\boldsymbol{r},\boldsymbol{r}')R_{\rm PS(V)}(\boldsymbol{r}',t), \tag{8}$$

where the first term in the left-hand side is responsible for the fully relativistic treatment for the kinetic term. For the S-wave mesons, the A_1^+ projection is supposed to be applied to the correlation functions defined above as $R_{\rm PS(V)}(\boldsymbol{r},t) \to R_{\rm PS(V)}(A_1^+;r,t)$. Starting from Eq. (8) with the same approximation on the nonlocal potential $U(\boldsymbol{r},\boldsymbol{r}')$, we thus obtain the alternative formula of $V_{\rm PS(V)}(r)$ as follows:

$$V_{\rm PS(V)}(r) = \frac{1}{m_Q}\frac{\boldsymbol{\nabla}^2 R_{\rm PS(V)}(r,t)}{R_{\rm PS(V)}(r,t)} - \frac{(\partial/\partial t)R_{\rm PS(V)}(r,t)}{R_{\rm PS(V)}(r,t)} + \frac{1}{4m_Q}\frac{(\partial/\partial t)^2 R_{\rm PS(V)}(r,t)}{R_{\rm PS(V)}(r,t)}\ . \tag{9}$$

We hereafter will omit the second derivative term of t in the analysis, being treated on the same footing as was done in Eq. (4).

Recall that the new method strongly relies on an assumption that there is a single unique potential to describe a series of the BS wave functions from the ground state to higher lying states. However, it is a non-trivial question whether the assumption is valid for the $Q\bar{Q}$ system. We would like to verify the validity of this method through a direct comparison of the interquark potentials, which are independently determined from the ground ($1S$) state and the radially excited ($2S$) state respectively.

3 Numerical results

The computation of the BS wave functions for the charmonium system is carried out on a lattice $N_s^3 \times N_t = 32^3 \times 64$ using the 2+1 flavor PACS-CS gauge configurations, where the simulated pion mass is closest to the physical point as $m_\pi = 156(7)$ MeV [17]. Simulation parameters of PACS-CS gauge configurations are summarized in Table 1. Our results are analyzed on all 198 gauge configurations, which are available through International Lattice Data Grid and the Japan Lattice Data Grid [1]. For the charm quark, we employ the relativistic heavy quark (RHQ) action that removes main discretization errors induced by large charm quark mass. The RHQ action, which is a variant of the Fermilab approach [18], is the anisotropic version of the $O(a)$ improved Wilson action (for details, see Refs. [19, 20]).

N_f	$N_s^3 \times N_t$	β	κ_{ud}	κ_s	a [fm] (a^{-1} [GeV])	$N_s a$ [fm]	M_π [MeV]	# configs.
2 + 1	$32^3 \times 64$	1.9	0.13781	0.13640	0.0907(13) (≈ 2.18)	2.90(4)	$\approx$156	198

Table 1. Parameters of the 2 + 1-flavor PACS-CS gauge configurations [17].

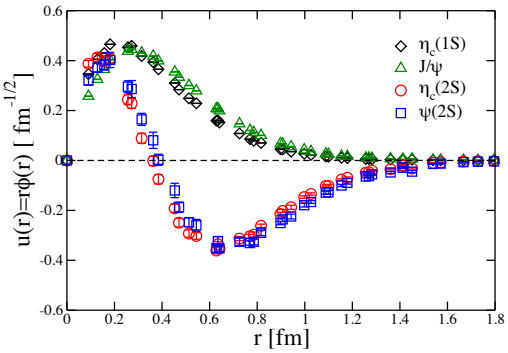

Figure 1. The reduced BS wave functions $u(r) = r\phi(r)$ for the $\eta_c(1S)$ (diamonds), J/ψ (upper triangles), $\eta_c(2S)$ (circles) and $\psi(2S)$ (squares) states, shown as a function of the spatial distance r. They are normalized as $\sum_{\boldsymbol{r}} |\phi(\boldsymbol{r})|^2 = 1$.

We first show the reduced BS wave functions $u_{n,\Gamma}(r) = r\phi_{n,\Gamma}(\boldsymbol{r})$ of both $1S$ and $2S$ charmonium states for displaying the spatial distribution of the BS wave function in Fig. 1. The wave functions displayed in Fig. 1 are normalized as $\sum_{\boldsymbol{r}} |\phi_{n,\Gamma}(\boldsymbol{r})|^2 = 1$. We plot data points taken along simpler $\boldsymbol{r}$ vectors, which are multiples of three directions, (1,0,0), (1,1,0) and (1,1,1), in order to avoid large discretization errors induced by the discrete Laplacian $\boldsymbol{\nabla}^2$ [11] in the later discussion. Both $1S$ and $2S$ wave functions are well localized and fitted enough in a (2.9 fm)^3 box. For the $2S$ states, the wave function exhibits a specific nodal structure around $r = 0.4$ fm.

[1] International Lattice Data Grid/Japan Lattice Data Grid, http://www.jldg.org.

Once determining the BS wave function, we are able to evaluate the interquark potentials via the time-independent (or time-dependent) method. While the kinetic quark mass is determinated within the BS amplitude method, the central and spin-spin potentials explicitly depend the kinetic quark mass as shown by Eqs. (2) and (3).

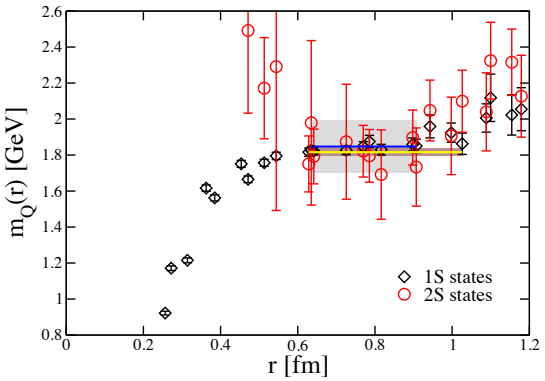

Figure 2. The determination of quark kinetic mass within the BS amplitude method. Horizontal solid lines indicate a value of quark kinetic mass obtained by fitting an asymptotic constant obtained from either $1S$ or $2S$ states. Shaded bands indicate fitting range and a statistical error estimated by the jackknife method.

method	Previous work [12]	Variational method	
type of source	Wall source	Gauss-smeared sources	
state	$1S$	$1S$	$2S$
m_Q [GeV]	1.784(23)	1.816(21)	1.847(145)
fit range	$[6 : 7\sqrt{3}]$	$[4\sqrt{3} : 8\sqrt{2}]$	[7 : 10]

Table 2. Summary of charm quark masses, which are determined from the BS amplitudes of both $1S$ and $2S$ charmonium states with their fit ranges $[r_{\rm min}/a : r_{\rm max}/a]$.

Figure 2 shows that asymptotic constants obtained from the right-hand side of Eq. (1). The black diamond and red circle represent the $1S$ state and $2S$ state determined from the each BS wave function independently. The constant behaviors from both results appear to be overlapped in the range of 0.6 fm $\lesssim r \lesssim$ 1.0 fm. We then obtain $m_Q(1S) = 1.816(21)$ GeV from the $1S$ wave functions and $m_Q(1S) = 1.847(145)$ GeV from the $2S$ wave functions by a constant fit over above r range with χ^2/d.o.f. < 2. These values are consistent with each other, and also with our previous work as listed in Table 2. It indicates that within the current precision a unique result for the quark kinetic mass is likely given regardless of the choice of either the ground- or excited-state pairs. This observation is highly consistent with success of potential description of the charmonium system.

Next, we show two independent results of the central potentials $V_C(r)$ using the BS wave functions of either $1S$ or $2S$ states in Fig. 3. In the left panel, we show "time-independent" results which are

independently evaluated for $1S$ and $2S$ states. The gross features of the resulting central potential $V_C^{2S}(r)$ from the $2S$ states are basically analogous to those of the $1S$ states $V_C^{1S}(r)$. However, some discrepancy beyond the quoted statistical errors appears in two specific regions: around $r = 0.4$ fm and at long distances ($r \gtrsim 1.1$ fm).

The origin of the former discrepancy can be attributed to the presence of a node in the $2S$ wave function, which is located at $r \approx 0.4$ fm as shown in Fig. 1. It should be reminded that the potential defined in the BS amplitude method is basically calculated by the second spatial derivative of the BS wave function divided by the BS wave function, $\nabla^2\phi_\Gamma/\phi_\Gamma$. Therefore, the potential can not be given only at nodes of the BS wave function.

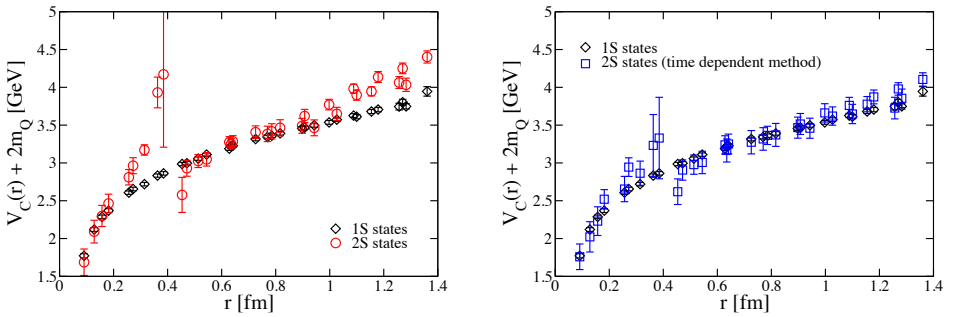

Figure 3. Left: Central (spin-independent) charmonium potentials calculated from the BS wave functions using the S-wave ground ($1S$) states and their first radially excited ($2S$) states. Right: Central (spin-independent) charmonium potentials from "time-independent" method for $1S$ states and "time-dependent" method for $2S$ states. For clarity of the figure, the "threshold energy value" $2m_Q$, that was encoded in the constant energy shift ($E^{nS}_{\rm ave} = M^{nS}_{\rm ave} - 2m_Q$), is not subtracted. Note that there is no adjustment parameter.

As for another discrepancy found at long distances, it should be simply because of the larger statistical uncertainties in the BS wave function of the higher-lying excited states. As shown in Fig. 1, the BS wave functions of both $1S$ and $2S$ states are localized around the origin and vanished at long distances. The signal-to-noise ratio on the quantity of $\nabla^2\phi_\Gamma/\phi_\Gamma$ becomes worse rapidly as the spatial distance r increases because of such localized nature of the BS wave functions. This tends to cause large systematic uncertainties at long distances, stemming from the choice of time window for the averaging process of $\nabla^2\phi_\Gamma/\phi_\Gamma$ over the time-slice range (for details of "time-average" procedure, see Ref. [11]). Time average for $\nabla^2\phi_\Gamma/\phi_\Gamma$ was performed in the range of $[t_{\rm min}/a : t_{\rm max}/a] = [24 : 33]$ for the $1S$ states and [7:12] for the $2S$ states. On the other hand, we show the central potential determined from "time-dependent method" in the right panel of Fig. 3. The fact that the discrepancy at long distances ($r \gtrsim 1.1$ fm) is improved indicates that the statistical uncertainties are relatively under control. We here choice the earlier time-fit range $[t_{\rm min}/a : t_{\rm max}/a] = [5 : 11]$ in the "time-average" procudure as an advantage of "time-dependent method". Consequently, we conclude that the charmonium potential $V_C^{2S}(r)$ exhibits the linearly rising potential at large distances and the Coulomb-like potential at short distances and is identical to $V_C^{1S}(r)$ within the current statistical precision.

Finally, we also determine the spin-spin potential from the BS wave functions of both $1S$ and $2S$ states. In Fig. 4, we compile three results of the spin-spin charmonium potential. The potential $V_S^{1S}(r)$ exhibits a repulsive interaction for spin-triplet states and an attractive interaction for spin-singlet states

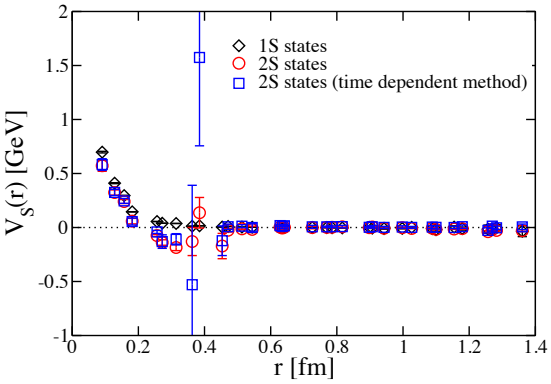

Figure 4. Spin-spin charmonium potentials from "time-independent" method for both $1S$ states (diamonds) and $2S$ states (circles) and also from "time-dependent" method for $2S$ states (squares).

with a finite range of $r \lesssim 0.6$ fm, which is the same as discussed in Ref [10, 12]. While the spin-spin potentials for $1S$ state and $2S$ state are also consistent with each other in the almost region, the small negative dip appear $0.3 \lesssim r \lesssim 0.4$ fm. This dip has the same origin with the divergence behavior of the central potential $V_C^{2S}(r)$. Thus, in the case of the spin-independent central potential, it is found that an application of the "time-dependent" method is certainly effective in the analysis of the $2S$ states.

4 Summary

We have calculated the BS wave functions for both the ground and first excited states of the S-wave charmonia (η_c and ψ mesons) in full lattice QCD. Our simulations have been carried out at almost physical point using 2+1 flavor PACS-CS gauge configurations ($M_\pi \approx 156$ MeV) with the RHQ action.

Applying the variational method to the $\boldsymbol{r}$-dependent two-point correlation function, we have evaluated the BS wave functions for the $1S$ and $2S$ states with spin singlet and triplet. Compared with the results of $1S$ states, the BS wave functions of both the $\eta_c(2S)$ and $\psi(2S)$ states exhibit a specific nodal structure in the radial direction.

We then have read off the value of the charm quark mass from the long-distance asymptotic value of the difference of "quantum kinetic energies", $\boldsymbol{\nabla}^2\phi_\Gamma/\phi_\Gamma$, between the members of hyperfine multiplets. It is found that the resulting charm mass is consistent regardless of the choice of either the ground- or excited-state pairs in the S-wave charmonia.

Using the kinetic quark masses as input, we have determined the spin-independent central potential $V_C^{2S}(r)$ and spin-spin potential $V_S^{2S}(r)$, which are basically analogous to those of the $1S$ states. The large discrepancies are limited in the particular region, where a subtlety is involved in the calculation of $\boldsymbol{\nabla}^2\phi_\Gamma/\phi_\Gamma$ due to almost zero value of ϕ_Γ that happens near the node of $\phi_\Gamma^{2S}(r)$ or at long distances with large statistical uncertainties. On the other hand, the statistical issues on $\phi_\Gamma^{2S}(r)$ is improved by the new "time-dependent" method which is applied only for the analysis of both $V_C^{2S}(r)$ and $V_S^{2S}(r)$.

The spin-independent central potential $V_C^{2S}(r)$ is identical to $V_C^{1S}(r)$ within the current statistical precision, while the discrepancy between the spin-spin potentials, $V_S^{1S}(r)$ and $V_S^{2S}(r)$, still remains more or less visible near the node location.

We thus conclude that a universal interquark potential and a unique quark mass can be simultaneously defined in a series of the BS amplitudes from the ground state to excited states. What this means is two-fold: 1) it ensures the reliability of the "time-dependent" approach in the BS amplitude method for the $Q\bar{Q}$ system and 2) it strongly supports the validity of the potential description for the charmonium system, at least, below open-charm threshold.

Acknowledgments

We thank the PACS-CS collaboration for making their 2+1 flavor gauge configurations available through ILDG/JLDG. Numerical calculations reported here were partially carried out on the COMA (PACS-IX) system at the CCS, University of Tsukuba, and LX406Re-2 at Cyberscience Center, Tohoku University.

References

[1] E. Eichten, K. Gottfried, T. Kinoshita, J. B. Kogut, K. D. Lane and T. M. Yan, Phys. Rev. Lett. **34**, 369 (1975); Erratum: [Phys. Rev. Lett. **36**, 1276 (1976)].
[2] S. Godfrey and N. Isgur, Phys. Rev. D **32**, 189 (1985).
[3] T. Barnes, S. Godfrey and E. S. Swanson, Phys. Rev. D **72**, 054026 (2005).
[4] G. S. Bali, Phys. Rept. **343**, 1 (2001).
[5] N. Ishii, S. Aoki and T. Hatsuda, Phys. Rev. Lett. **99**, 022001 (2007).
[6] S. Aoki, T. Hatsuda and N. Ishii, Prog. Theor. Phys. **123**, 89 (2010).
[7] Y. Ikeda and H. Iida, PoS LATTICE **2010**, 143 (2010).
[8] Y. Ikeda and H. Iida, Prog. Theor. Phys. **128**, 941 (2012).
[9] T. Kawanai and S. Sasaki, Phys. Rev. Lett. **107**, 091601 (2011).
[10] T. Kawanai and S. Sasaki, Phys. Rev. D **85**, 091503 (2012).
[11] T. Kawanai and S. Sasaki, Phys. Rev. D **89**, no. 5, 054507 (2014).
[12] T. Kawanai and S. Sasaki, Phys. Rev. D **92**, no. 9, 094503 (2015).
[13] C. Michael, Nucl. Phys. B **259**, 58 (1985).
[14] M. Lüscher and U. Wolff, Nucl. Phys. B **339**, 222 (1990).
[15] K. Nochi, T. Kawanai and S. Sasaki, Phys. Rev. D **94**, no. 11, 114514 (2016).
[16] N. Ishii *et al.* [HAL QCD Collaboration], Phys. Lett. B **712**, 437 (2012).
[17] S. Aoki *et al.* [PACS-CS Collaboration], Phys. Rev. D **79**, 034503 (2009).
[18] A. X. El-Khadra, A. S. Kronfeld and P. B. Mackenzie, Phys. Rev. D **55**, 3933 (1997).
[19] S. Aoki, Y. Kuramashi and S. i. Tominaga, Prog. Theor. Phys. **109**, 383 (2003).
[20] Y. Kayaba *et al.* [CP-PACS Collaboration], JHEP **0702**, 019 (2007).